2002.

Late Quaternary turbidite input into the east Mediterranean basin: new radiocarbon constraints on climate and sea-level control

MICHAEL S. REEDER[1], DORRIK A. V. STOW[1] & R. GUY ROTHWELL[2]
[1]*School of Ocean and Earth Sciences, University of Southampton, Southampton Oceanography Centre, European Way, Southampton SO14 3ZH, UK*
(e-mail: davs@soc.soton.ac.uk)
[2]*Challenger Division for Seafloor Processes, Southampton Oceanography Centre, European Way, Southampton SO14 3ZH, UK*

Abstract: The Late Pleistocene–Holocene (0–30 ka BP) allochthonous sedimentation in the Herodotus Basin of the eastern Mediterranean has been controlled, in part, by a combination of regional climatic change and eustatic sea-level fluctuation. A new series of radiocarbon dates, made on planktonic foraminifers and pteropod shells taken from the pelagic and hemipelagic intervals between individual turbidite units, has given bracketing dates for each major turbidity current event that deposited sand and mud on the Herodotus Basin plain. Two partly independent cycles are evident. Climate-induced cycles have lead to an alternation of periods of turbidites sourced from the Nile delta–fan system with those from the North African shelf and Anatolian rise. These correlate with pluvial and inter-pluvial climatic periods recognized in the Nile hinterland. Sea-level cycles have tended to focus turbidite emplacement, from whatever source, at periods of sea-level fall within the latest Wisconsin and sea-level rise from the Wisconsin–Holocene period. In addition to the Herodotus Basin Megaturbidite (HBM) described previously, six other beds with volumes in excess of 25 km^3 and wide lateral extent across the basin can be termed megaturbidites. There is no simple sea-level or climate control on the timing of these events, so we must conclude that triggering and emplacement of megaturbidites is independent and variable.

The Herodotus Basin is a SW–NE-trending elongate depression that lies to the NW of the Nile Cone and has a maximum water depth in excess of 3000 m. It is the largest basin in the eastern Mediterranean, with the 3000-m isobath delineating an area of approximately 27 000 km^2. The detailed physiography of the basin is presented by Reeder *et al.* (1998, 2000), who have calculated the areal extent of Late Pleistocene ponded sediment to be in the order of 40 000 km^2 (Fig. 1). This is significantly greater than the area based on the 3000-m isobath, as sediment has overspilled this level by up to at least 2700 m in places.

Herodotus Basin sedimentation

The Late Pleistocene sedimentary characteristics of the Herodotus Basin are reported in detail by Cita *et al.* (1984), Lucchi & Camerlenghi (1993) and Reeder *et al.* (1998, 2000). The most recent work by Reeder *et al.* (1998, 2000) was based on a longitudinal basin transect of five giant piston cores, collected on the *Marion Dufresne* Cruise 81 (Table 1). These cores penetrated to a maximum depth of 24.2 m and emplacement of the oldest sediments was estimated at less than 30 ka BP. Hence, all the sediments are from the Late Pleistocene and mainly comprise turbidites from four discrete sediment sources (Fig. 1). Individual turbidites are readily correlated between cores across the Herodotus Basin on the basis of their particular compositional characteristics. Sources have been determined both by mineralogical content (Cita *et al.* 1984; Lucchi & Camerlenghi 1993) and by the measured decrease of turbidite and sand-fraction thicknesses with increased transportation (Reeder *et al.* 1998). Individual turbidites have been named 'a'–'p', where 'a' represents the youngest and 'p' the oldest of the events.

Some 50% of the named turbidites were derived from an organic-rich Nile Cone source. These have

From: JONES, S. J. & FROSTICK, L. E. (eds) 2002. *Sediment Flux to Basins: Causes, Controls and Consequences.* Geological Society, London, Special Publications, **191**, 267–278. 0305-8719/02/$15.00

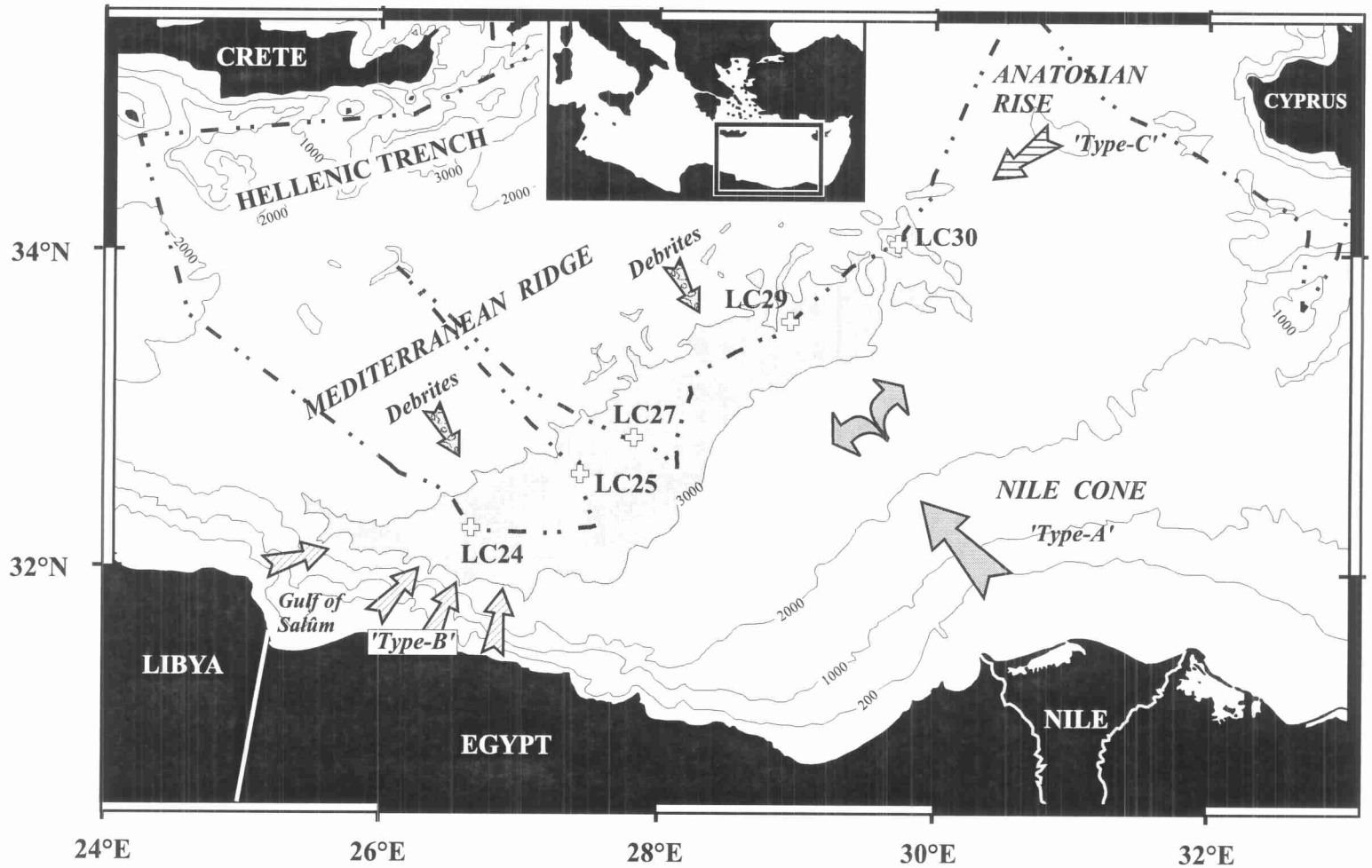

Fig. 1. Location of the Herodotus Basin, showing the main sediment sources, core positions and the navigational track of the *Marion Dufresne* Cruise 81 (MD81).

Table 1. *Water depth, positions and lengths for the five long-piston cores collected during* Marion Dufresne *Cruise 81 (MD81)*

Core No.	Water depth (m)	Latitude	Longitude	Core length (m)
LC24	3191	32°17.71′N	26°37.95′E	18.31
LC25	3129	32°36.01′N	27°23.25′E	13.71
LC27	3131	32°48.91′N	27°40.45′E	14.95
LC29	3138	33°35.63′N	28°56.32′E	24.66
LC30	3144	34°04.70′N	29°42.72′E	25.82

been termed 'Type A' turbidites, following the nomenclature of the first description of allochthonous sediments in the basin by Cita *et al.* (1984). They range from 15 to 750 cm in thickness and are fine-grained turbidites with thin (maximum of 30 cm thick) silty and sandy bases. Estimates of their total volume range from 0.1 to 126 km^3, with a possible maximum for one of the deepest turbidites 'o' of around 190 km^3 (Reeder *et al.* 1998). The second most abundant source is the NE African shelf ('Type B' turbidites) with thicknesses ranging from 6 cm to over 16 m (Fig. 2), and estimated volumes from 0.1 to 400 km^3. The largest of these, turbidite 'n' is referred to as the Herodotus Basin Megaturbidite (HBM). These more carbonate-rich (typically 40–50 % $CaCO_3$) sediments are easily recognizable from their Nile Cone counterparts by their lighter coloration. The light olive–grey 'Type B' turbidites reflect a relative abundance of carbonate shelf organisms, whilst the 'Type A' Nile Cone-derived turbidites are dark brown–grey and reflect an abundance of plant and other terrigenous material. Two further discrete sources have been described by Reeder *et al.* (1998), being 'Type C' turbidites derived from the Anatolian Rise to the NE of the Herodotus Basin, and the debris flow deposits (debrites) from the Mediterranean Ridge on the northern flank of the basin (Fig. 1).

The petrology, geochemistry, correlation and stratigraphy of Late Pleistocene sedimentation in the Herodotus Basin are presented in detail elsewhere (Cita *et al.* 1984; Lucchi & Camerlenghi 1993; Reeder *et al.* 1998, 2000) and summarized partially here in Fig. 2. Although the Late Pleistocene stratigraphy of the Herodotus Basin is known in general terms, precise dating of individual turbidite events, and hence elucidation of their relationship with climatic change and eustatic sea-level fluctuation, has not previously been attempted. The nannofossil zonation reported previously indicates that all turbidites were deposited within the last 60 ka. The thickness of hemipelagic accumulation between turbidites was then used to estimate tentative emplacement dates for all event deposits, thereby concluding that the oldest sediments recovered were around 30 ka (Reeder *et al.* 1998).

In this paper we present absolute dates for turbidite emplacement on the Herodotus Basin plain, based on radiocarbon dating of the pelagic and hemipelagic intervals between turbidites. These are then discussed in relation to climatic changes and fluctuation in eustatic sea level during the latest Pleistocene.

AMS radiocarbon (^{14}C) dating

By sampling the planktonic foraminifera from pelagic horizons overlying and underlying turbidites, bracketing emplacement dates were obtained for each event. The AMS radiocarbon dating method of Thomson & Weaver (1994) was used, which entailed sampling the whole of the pelagic interval, as well as the top 10–15 cm of the underlying turbidite, in order to include any forams reworked by burrowing fauna. A continuous trench sampling technique was employed.

In total, 10 samples were collected from the Herodotus Basin cores, at the core depths shown in Fig. 2. Larger planktonic foraminifera are expected to be the least susceptible component of the pelagic interval to be redistributed by currents and thus the most suitable for dating. Samples were therefore sieved to obtain the >150-μm size fraction, and the clean planktonic foraminifera and pteropods were selected from this. All other bioclastic and lithic material, together with forams and pteropods contaminated with sediment, were removed from the >150-μm sieved fraction by hand picking.

Corrections to the raw ^{14}C dates were made to account for the relationship between the radiocarbon and calendar timescales by applying the correction factor of:

$$\text{Calendar years} = 1.24 \times (^{14}\text{C years}) - 440$$

(Bard *et al.* (1993) (Table 2). The values include a correction of 400 years to account for the offset ^{14}C age of the atmospheric and oceanic mixed-layer reservoir (Stuiver 1990).

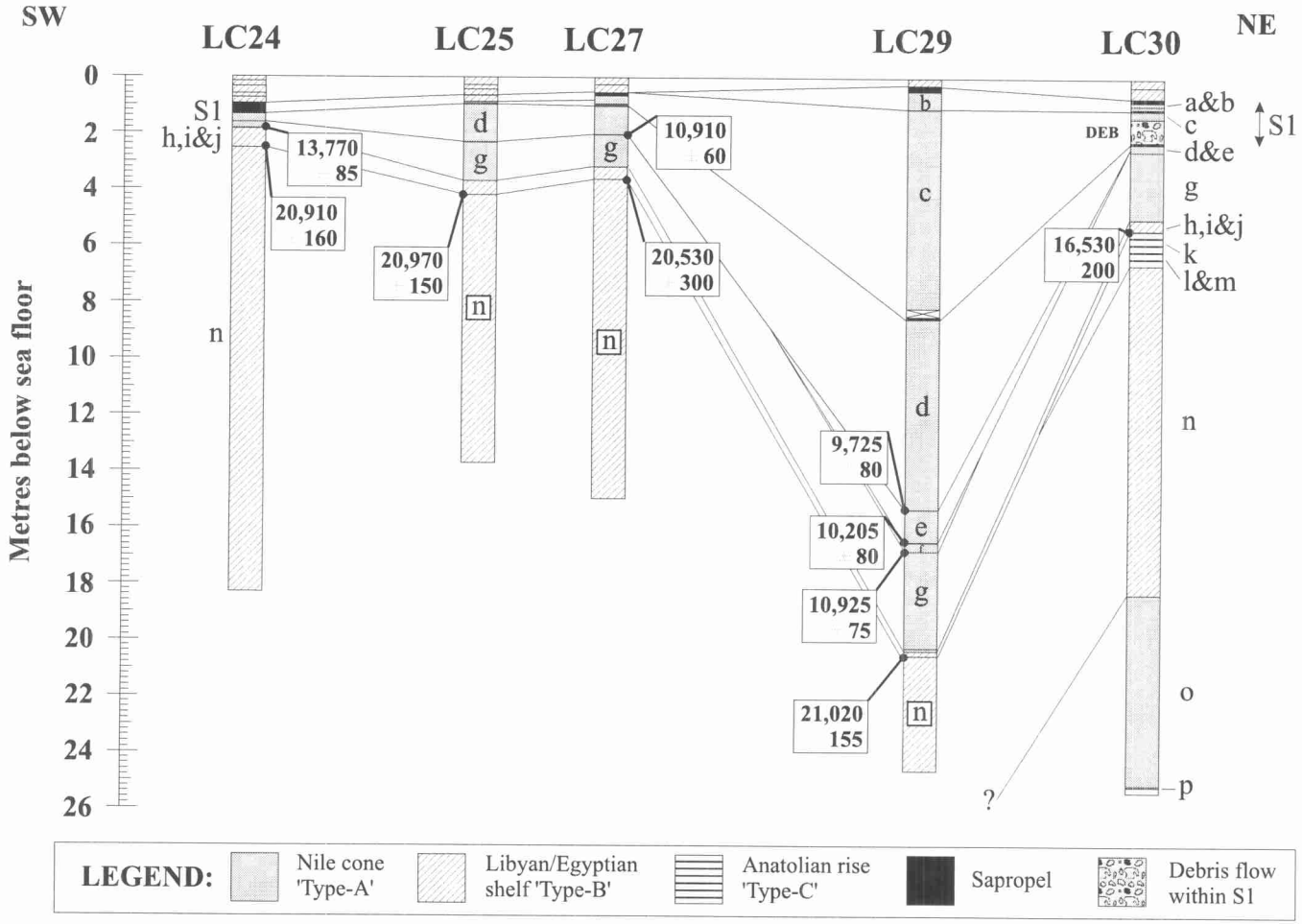

Fig. 2. Stratigraphy, correlation and conventional radiocarbon dates of sediments in the five long-piston cores from the Herodotus Basin. Note: The transect from LC24 to LC30 is approximately 325 km in length.

Table 2. *Details from the AMS ^{14}C dating of the 10 samples from the Herodotus Basin cores, with calculated calendar ages*

Publication code	Sample identifier	^{14}C enrichment (% modern ± 1σ)	Carbon content (5 dry wt)	$\delta^{13}C_{PDP}$ ±0.1 0/00	$\delta^{18}O_{PDP}$ ±0.1 0/00	Convetional radiocarbon age (years BP ± 1σ)	Calculated calendar age* (years BP)
AA-24162	LC29.7.83-99	29.80 ± 0.30	10.2	0.1	1.3	9725 ± 80	11 620
AA-24163	LC29.6.64-77	28.07 ± 0.28	n/a	0.4	n/a	10 205 ± 80	12 215
AA-24164	LC29.6.873-100	25.66 ± 0.25	10.7	–0.3	3.1	10 925 ± 75	13 105
AA-24165	LC29.3.18-31	7.30 ± 0.15	n/a	–1.5	n/a	21 020 ± 155	25 625
AA-24166	LC25.7.62-75	7.35 ± 0.15	10.2	1.4	3.1	20 970 ± 150	25 565
AA-24167	LC27.9.49-64	7.76 ± 0.29	10.6	1.5	3.4	20 530 ± 300	25 015
AA-24168	LC30.16.105-116	12.77 ± 0.32	10.7	1.2	3.7	16 530 ± 200	20 055
AA-24169	LC24.13.10-25	18.02 ± 0.20	9.7	1.3	2.7	13 770 ± 85	16 635
AA-24170	LC24.13.49-63	7.40 ± 0.15	10.5	1.5	3.7	20 910 ± 160	25 490
CAMS-388650	LC27.10.22-53	25.71 ± 0.17	10.6	0.7	1.3	10 910 ± 60	13 090

*Following the correction of Bard *et al.* (1993), where: Calendar age = 1.24 × (^{14}C age) –440.

Turbidite emplacement vs sea level

The results of the radiocarbon dating are presented in Fig. 3. By bracketing the emplacement of the turbidite an average date has been obtained for each event (Table 3). We can identify four distinct periods of time characterized by cyclic differences in turbidite source and then compare these with the eustatic sea-level curve (Fig. 3) (Haq *et al.* 1987).

Sea-level low-stand (pre-28 ka BP)

Only two turbidites from the present core suite (core LC30) fall within this time period, and both of these are Type-A turbidites from the Nile source. Stanley & Maldonado (1979) also reported Nile-derived turbidites between 55 and 28 ka BP, relating to a transgressive period of slightly higher sea level within the main Wisconsin low stand system tract. Based on the limited data available in these earlier studies, we estimate a relatively low average accumulation rate of between 0.02 and 0.05 m ka^{-1} during this interval.

Lowering sea level (28–17 ka BP)

By contrast, the Late Wisconsin regression, when sea level dropped to its lowest value of around 125 m below present depths, is characterized by an absence of Type A turbidites. This period begins with deposition of the Herodotus Basin Mega-turbidite (Type B) at just over 27 ka, followed by three smaller volume Type C turbidites from a northern source (Anatolian Rise), and then three small Type B turbidites from the North African margin. Although the numbers are somewhat limited, this represents turbidite emplacement on to the basin plain of one event every 1.4 ka approximately. The thickness of the megaturbidite can be estimated at just over 20 m proximally, decreasing to some 12.5 m where the base was cored at site LC30. This clearly makes up the major part of an average accumulation rate of between 1.3 and 2 m ka^{-1}.

Rising sea level (17–6 ka BP)

Following the lowest sea-level stand of the last glacial (around 18–17 Ma BP), the pattern of sedimentation changed notably as sea level rose rapidly at a rate of approximately 12.5 m ka^{-1} (1.25 cm a^{-1}). During this period, and in contrast to the period preceding the glacial, the Herodotus Basin stratigraphy was dominated by thicker Nile Cone-derived turbidites (Type A), rather than the thin North African shelf and Anatolian Rise-derived turbidites.

The Nile Cone received very large quantities of sediment and entered a period of major accumulation (Mart 1993). Several of the larger-scale turbidity currents bypassed the fan to reach the basin plain, entering the relatively flat basin adjacent to the location of core station LC29. This is reflected in the thickest accumulation of Type A turbidites centred around this area (Fig. 2) and also indicated by 3.5 kHz seismic evidence of distributary channels in this vicinity (Reeder *et al.* 1998). Towards the end of the sea-level rise, anoxic bottom water conditions occurred across the eastern Mediterrranean basin leading to deposition of the organic-rich S1 sapropel. During this period only small-volume Nile Cone turbidites ('a', 'b' and 'c') were deposited, continuing the pattern of mono-source input on the Herodotus Basin plain. Turbidites reached the basin plain on average once every 1.8 ka during this phase of rising sea level, giving an accumulation rate of 1.82 m ka^{-1} in the main depocentre (core LC29) and only some 0.1 m ka^{-1} at the SW end of the basin (core LC24).

Sea-level high-stand (6–0 ka BP)

The record of sedimentation after the deposition of the S1 sapropel is poorly preserved in the MD81 cores. There is an inherently large amount of deformation caused by the piston coring technique, which may have removed a small quantity of the most recent sediments. However, the sequence observed is dominated by the presence of thin Type B turbidites (un-named) and thin hemipelagic intervals (Fig. 2). Turbidite emplacement varied from one event in 6 ka to one event every 1.5 ka, and the average rate of accumulation from 0.07 to 0.15 m ka^{-1}.

Summary

The most apparent relationship between turbidite emplacement and sea-level is an increase in the thickness of turbidites reaching the Herodotus Basin plain, and hence in the average rate of accumulation, during both the Late Wisconsin sea-level fall to its lowest stand and the Late Wisconsin–Holocene sea-level rise. In the former period the turbidites were exclusively Types B and C, whereas in the latter period they were Nile Type A.

Turbidite emplacement vs climate

Considering the same four periods of time, we can consider instead the climatic variation that may also have had some effect on both the rate of turbidite supply and the source of sediment (turbidite type). The principal variation likely to affect sedimentation is between pluvial and inter-pluvial episodes

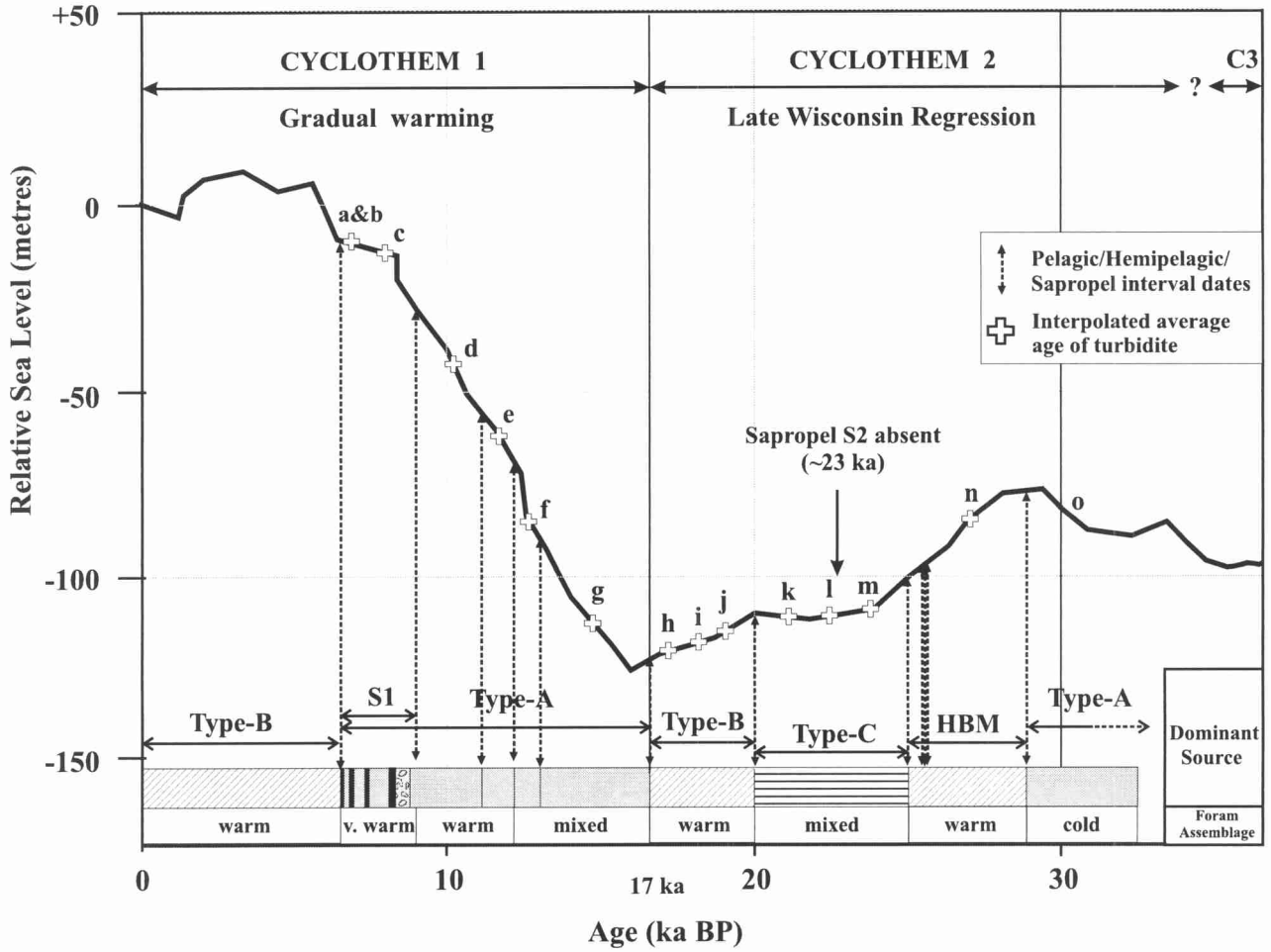

Fig. 3. Eustatic sea-level curve for the past 30 ka (after Shackleton 1987) showing individual turbidites as well as turbidite types based on source area. Two possible cyclothems are indicated, but see text for discussion. Foram assemblages after Kahler & Dossi (1996).

Table 3. *Interpolated depositional ages for the Late Pleistocene Herodotus Basin turbidites*

Turbidite	Type	Approximate volume*	Age of overlying dated pelagic interval (years BP)	Age of underlying dated pelagic interval (years BP)	Interpolated depositional age† (years BP)
Turbidite 'a'	A	0.1			7000
Turbidite 'b'	A	6.0	6500 (S1)	9500 (S1)	7500
Turbidite 'c'	A	80.0			8000
Debrite		2.4			8500
Turbidite 'd'	A	126.0	9500 (S1)	11 620	10 560
Turbidite 'e'	A	25.2	11 620	12 215	11 920
Turbidite 'f'	A	0.1	12 215	13 105	12 660
Turbidite 'g'	A	72.0	13 105	16 635	14 870
Turbidite 'h'	B	2.2			17 490
Turbidite 'i'	B	0.8	16 635	20 055	18 345
Turbidite 'j'	B	0.8			19 200
Turbidite 'k'	C	8.0			21 400
Turbidite 'l'	C	0.04	20 055	25 425	22 740
Turbidite 'm'	C	4.0			24 740
Turbidite 'n'	B	400	25 425[HBM]	28 825[HBM]	27 125[HBM]
Turbidite 'o'	A	190?	28 825	?	>28 825
Turbidite 'p'	B	0.1?	?	?	?

*Volumes from Reeder *et al.* (1998).
†Mean date of the overlying and underlying pelagic intervals.
[HBM]Dates for the Herodotus Basin Megaturbidite.

that brought alternately wetter and drier conditions, respectively, to the upper reaches of the Nile River (or Neonile as the Late Pleistocene river is generally known) (Said 1990). These were not exactly time equivalent to interglacial and glacial climatic intervals.

Kubbanivan pluvial (c. 50–28 ka)

The earliest period represented by our sediment records from the Herodotus Basin fell during the Kubbanivan pluvial episode – a relatively wet but still quite cold period. The Neonile would have carried much sediment to the delta region, thus providing an adequate source for downslope resedimentation by turbidity currents. The Herodotus Basin turbidites recovered from this period are all Type A (Nile-source).

Interpluvial (c. 28–17 ka)

During this period, the climate in the Nile hinterland was cold and dry, and much less sediment would have been supplied to the Nile Delta. The river was subject to rare storm-related flooding, but otherwise lower discharge. No Nile-derived turbidites reached the Herodotus Basin during this period, which is characterized by Type B (North African shelf) and Type C (Anatolian) turbidites only.

Nabtian pluvial (c. 17–6 ka)

Following the Late Wisconsin glacial maximum, the climate of the region began to ameliorate and the vegetation pattern changed from a cold, dry ecosystem to a humid, lake and marsh environment dominated by a herbaceous flora (Cheddadi *et al.* 1991; Cheddadi & Rossignol-Strick 1995). This pluvial period also led to an increase in sedimentary output onto the Nile Cone as a direct result of increased precipitation in the Nubian Massif (Ethiopian highlands) to the south. There is still uncertainty about the exact timing of climate change in the region, with some authors supporting more arid conditions in parts of the Nile drainage basin from 13 to 10 ka (Cheddadi & Rossignol-Strick 1995). The Nabtian pluvial *sensu stricto* is fairly well documented and generally considered to have lasted for a rather shorter time period, from about 10 to 5 ka, and to include three much shorter dry episodes (Said 1990). The generally more humid conditions and increased vegetation cover are confirmed by the high organic detritus content recorded in sediments collected from the Nile Cone and Herodotus Basin dating from this period (Ross *et al.* 1978; Cita *et al.* 1984; Lucchi & Camerlenghi 1993). The turbidites are all of Type A (Nile source).

Also, at approximately 10 ka BP reforestation occurred in the hinterlands of the Mediterranean, leading to a rejuvenation in supply of nutrients to the eastern Mediterranean basin (Cheddadi *et al.*

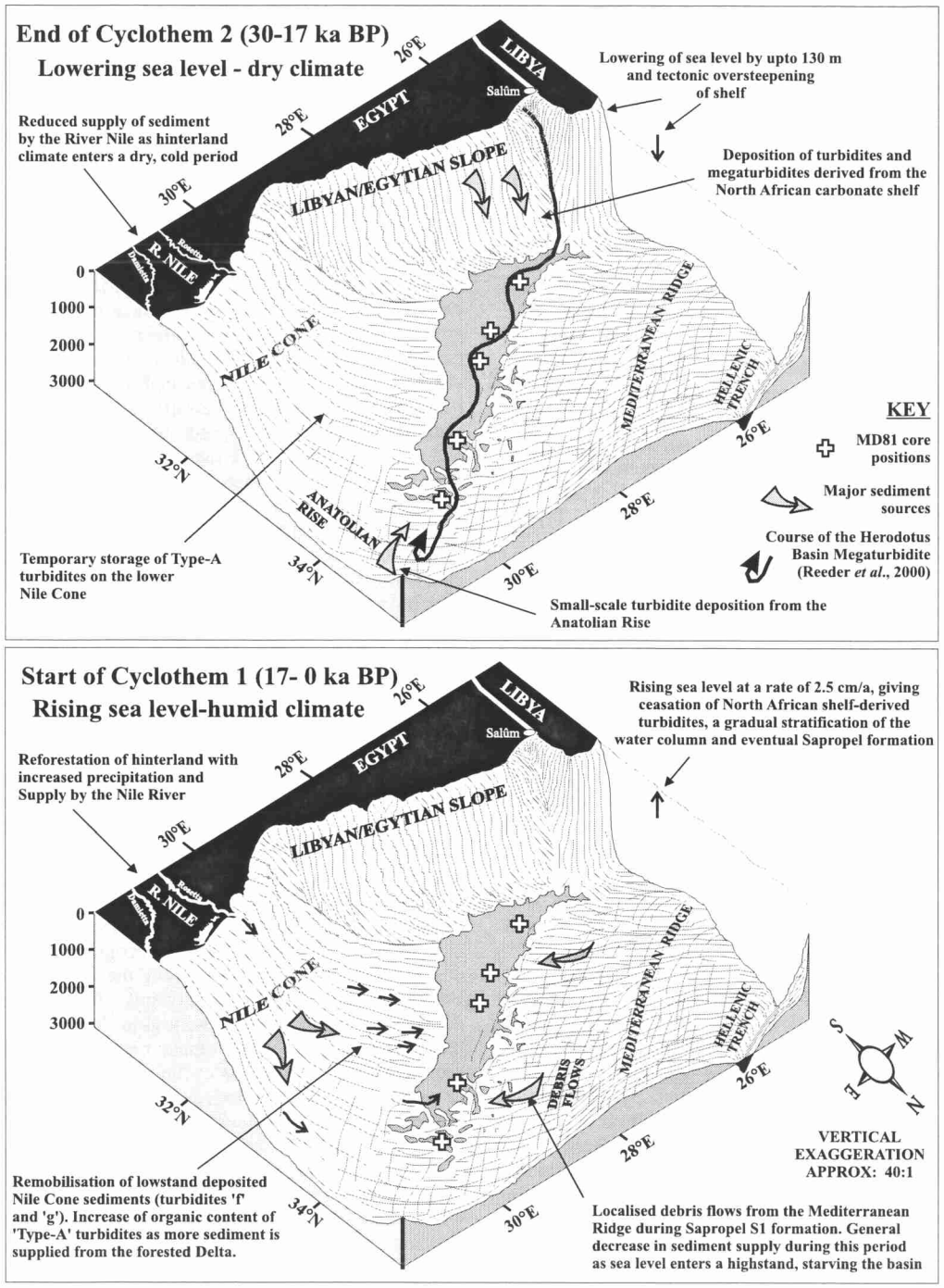

Fig. 4. Three-dimensional schematic box models for the climate-controlled variation in source for Herodotus Basin turbidites over the past 30 ka. (**a**) During the period from 30 to 17 ka, the stratigraphy is dominated by 'Type B' and 'Type C' turbidites, derived from the North African shelf and slope and the Anatolian Rise, respectively. This correlates with a dry, inter-pluvial climate. (**b**) During the period from 17 to 0 ka, the sequence is dominated first by rejuvenated sedimentary discharge from the River Nile, with 'Type A' turbidites abundant in the Herodotus Basin cores, and then later by reduced sedimentation during the Late Holocene.

1991). An increase of fresh water from influxes of snowmelt and river discharge is thought to have caused a disruption to the thermohaline currents of the Levantine and Ionian Seas, and initiated an increase in the primary productivity (Maldonado & Stanley 1978; Stanley & Maldonado 1979; Bethoux 1993; Rohling 1994; Higgs *et al.* 1994; Aksu *et al.* 1995). Stratification of the water column occurred, leading to stagnation of the bottom waters and deposition of the organic-rich sapropel S1 at the very end of this period.

Holocene inter-pluvial (6 – 0 ka)

The climate of the North African margin and Nile hinterland has remained fairly constant since about 6 ka BP, with very warm and arid conditions prevailing. Less material was supplied to the Nile Delta leading to lower rates of accumulation on the Nile Cone and an absence of Type A turbidites from the Herodotus Basin. Only thin Type B turbidites have been recovered.

Summary

There seems to be a clear relationship between turbidite type, indicative of sediment source, and climatic conditions. Pluvial episodes provided greater influx from the Nile River system to the Nile Delta. This in turn lead to greater downslope resedimentation to the Herodotus Basin. By contrast, the inter-pluvial episodes saw an absence of Nile-derived turbidites and dominance of the carbonate-rich North African shelf and Anatolian sources.

It is interesting to note, however, that foraminiferal assemblages from all types of turbidite show generally warm-water conditions post-28 ka BP, except for turbidites 'f' and 'g', which show mixed cold–warm assemblages (Kahler & Dossi 1996). Turbidite 'o', dating from around 30 ka BP, shows a complete cold assemblage of planktonic foraminifers, demonstrating deposition during the height of the Wisconsin glacial. The two mixed assemblage turbidites may result from the mixing of warm- and cold-water forms, at least one of which would have been reworked older turbidites or hemipelagic sediments deposited during different climatic conditions.

Discussion

Sediment cyclicity and controls

Based on an analysis of 65 piston and gravity cores, which collectively penetrated up to 55 ka into the Nile cone record, Maldonado & Stanley (1976, 1978) and Stanley & Maldonado (1979) noted a cyclic repetition of sedimentary facies, which they correlated with variations in the palaeo-climate and sea level. The timing of their three cycles or cyclothems more or less correlates with our broad temporal divisions based on turbidite types, although they recognize only Nile-derived turbidites. For Cycle 3 (55–28 ka) they record from base-up relatively fine-grained turbidites, sapropel 3, fine-grained turbidites and hemipelagites, and a calcareous ooze. Cycle 2 has coarser-grained turbidites, sapropel 2, turbidites/hemipelagites and calcareous ooze. Cycle 1 shows, once more, fine-grained turbidites, sapropel 1, hemipelagites and calcareous ooze. They do note that these cycles vary in detail between cores and regions, some being more dominated by hemipelagic and pelagic sediments ('suspensites') and some by turbidites and associated downslope facies ('gravitites').

In comparing the Herodotus Basin data with those described above mainly from the Nile Cone, we could consider the post-17 ka sequence of the Herodotus Basin as a single cyclothem (Fig. 3) consisting of three main constituents: (1) a lower dark brown–grey and turbidite-dominated sequence (Type A, Nile-derived) with thin hemipelagic muds, overlain by (2) a dark grey–black sapropelic layer (S1), and (3) an upper pale olive–grey mud section with thicker hemipelagic muds and thin turbidites (Type B, African shelf-derived). This sequence is, at first sight, similar to Cycle 1 of Stanley & Maldonado (1979), although the thin upper turbidites are from a different source. Possible earlier cyclothems (Fig. 3) are still less comparable, in that the lowermost Type A turbidites are not fully penetrated, the overlying sapropel (S2) is missing and the pale-coloured turbidites are from two different sources.

Therefore, although we do recognize some degree of cyclicity in cores from the Herodotus Basin, the cycles differ significantly from those described previously from the region. We suggest that both sea level and climate have influenced sedimentation, but that the cyclic response to each control has been partly independent. The climate-induced cycles are principally an alternation of periods dominated by Nile-sourced, organic-carbon-rich, muddy turbidites (Type A) and periods during which turbidites were derived from elsewhere, notably from North African and Anatolian biogenic, carbonate-rich, sources (Type B and Type C turbidites). These periods appear to correspond closely with pluvial and inter-pluvial episodes, respectively, that affected the African–Nile hinterland (Fig. 4).

Sea-level induced cycles are less evident, although from the data we have it would appear that turbidity current input into the Herodotus Basin,

from whatever source, was especially common during both falling and rising sea level. In particular, sea-level fall to the latest Wisconsin low-stand is characterized by turbidites derived from the North African shelf and Anatolian sources, including the Herodotus Basin Megaturbidite, whereas sea-level rise through the Late Wisconsin–Holocene is characterized by Nile-derived turbidites. Only the most recent Holocene period (post-6 ka) has fewer and thinner turbidites and more pelagic–hemipelagic sedimentation.

We cannot comment on sapropel cyclicity, but note that whereas sapropel S1 is well developed throughout the basin, sapropel S2 is absent from all basin cores. This seems more likely to be because it was never deposited than subsequently eroded, as the only turbidity current capable of eroding such a layer over a distance of at least 400 km is the HBM. Current dating puts the HBM event several thousands of years prior to S2.

Megaturbidites

Much has been written in the past 30 years on very large-scale turbidites – variously called megaturbidites or megabeds – and yet still no generally accepted rigorous definition exists. In our recent paper on the Herodotus Basin Megaturbidite (Reeder *et al.* 2000) we do comment on this problem but still prefer to steer away from too quantitative a definition at this stage. The early definitions of >1 m thick or >1 km^3 (Ricchi Lucchi & Valmori 1980; Mutti *et al.* 1984) are both too small in light of recent work on modern examples. The HBM, for example, is up to 20 m thick and some 400^3 km in volume. In fact, 10 of the 16 turbidites in this study might also be considered as megaturbidites as they display total sediment volumes in excess of 1 km^3, and six of these have volumes in excess of 25 km^3. This is perhaps typical of basin plain turbidite systems. We propose the following as a working definition, without placing strict limits on bed dimensions.

A *megaturbidite* is a generic term that describes a very thick, large-volume sedimentary unit (or bed), with a large areal extent, that has been deposited by a single turbidity current event. The principal characteristics of such beds are: (1) they are very thick in comparison with associated turbidites, at least in some part of the basin; (2) they have a very large volume, again relative to the associated turbidites; and (3) they are laterally extensive and, hence, tend to make good stratigraphic and seismic marker beds. This definition incorporates most of the qualitative characteristics for megaturbidites proposed by Bouma (1987), although we do not agree that they must be of 'different composition from the host rock', nor that they must necessarily 'lack submarine fan geometries'.

The HBM was deposited at about 27.1 ka BP during a period of lowering sea level from an already glacial low-stand. Of the other megaturbidites revealed in this study, turbidite 'o' was also deposited during the Wisconsin low-stand, whereas turbidites 'g', 'e', 'd' and 'c' occurred during rising sea level, the last two at the onset of the Holocene. In Reeder *et al.* (2000) we concluded that a combination of factors caused the catastrophic slope collapse that led to emplacement of the HBM, including lowered sea level leading to sediment destabilization, a weak glide plane horizon within the sedimentary succession on an over-steepened slope and a probable seismic trigger. Clearly not all these factors could have contributed to deposition of the other megaturbidites, and others may have been involved instead. It is reasonable to conclude, therefore, that the triggering and emplacement of megaturbidites is very variable, and that individual events occur independently of a particular sea-level stand or climatic condition.

The authors would like to thank the NERC Scientific Services, Radiocarbon Laboratory, East Kilbride, for their support in obtaining the radiocarbon dates (^{14}C Dating Allocation No. 664/0896). Thanks also to NERC's British Ocean Sediment Core Repository (BOSCOR) based at the SOC, where description and sampling was completed. M. S. Reeder's PhD is NERC funded: grant GT4/95/288/E. This work was supported by the European Union Marine Science and Technology Programme contract No. MAS2-CT93-0051.

References

AKSU, A. E., YASAR, D. & MUDIE, P. J. 1995. Paleoclimatic and paleoceanographic conditions leading to development of sapropel layer S1 in the Aegean Sea. *Palaeogeography, Palaeoclimatology, Palaeoecology*, **116**, 71–101.

BARD, E., ARNOLD, M., FAIRBANKS, R. G. & HAMELIN, B. 1993. ^{230}Th-, ^{234}U and ^{14}C obtained by mass spectrometry on corals. *Radiocarbon*, **35**, 191–199.

BETHOUX, J.-P. 1993. Mediterranean sapropel formation, dynamic and climatic viewpoints. *Oceanologica Acta*, **16**, 127–133.

BOUMA, A. H. 1987. Megaturbidite: an acceptable term? *Geo-Marine Letters*, **7**, 63–67.

CHEDDADI, R. & ROSSIGNOL-STRICK, M. 1995. Eastern Mediterranean quaternary paleoclimates from pollen and isotopic records of marine cores in the Nile cone area. *Paleoceanography*, **10**, 291–300.

CHEDDADI, R., ROSSIGNOL-STRICK, M. & FONTUGNE, M. 1991. Eastern Mediterranean palaeoclimates from 26 to 5 ka B.P. documented by pollen and isotopic analysis of a core in the anoxic Bannock Basin. *Marine Geology*, **100**, 53–66.

CITA, M. B., BEGHI, C., CAMERLENGHI, A., KASTENS, K.

A., McCoy, F. W., Nosetto, A., Parisi, E., Scolari, F. & Tomadin, L. 1984. Turbidites and megaturbidites from the Herodotus Abyssal Plain (Eastern Mediterranean) unrelated to seismic events. *Marine Geology*, **55**, 79–101.

Haq, B. U., Hardenbol, J. & Vail, P. P. 1987. Chronology of fluctuating sea levels since the Triassic. *Science*, **235**, 1156–1166.

Higgs, N. C., Thomson, J., Wilson, T. R. S. & Croudace, I. W. 1994. Modification and complete removal of Eastern Mediterranean sapropels by postdepositional oxidation. *Geology*, **22**, 423–426.

Kahler, G. & Dossi, M. 1996. Micropalaeontology. *In*: Rothwell, R. G. (ed.) R/V Marion Dufresne *Cruise 81 – Mediterranean Giant Piston Coring Transect*. Cruise Report, **40–63**.

Lucchi, R. & Camerlenghi, A. 1993. Upslope turbiditic sedimentation on the southeastern flank of the Mediterranean ridge. *Bollettino di Oceanologia Teorica ed Applicata*, **11**, 3–25.

Maldonado, A. & Stanley, D. J. 1976. The Nile Cone: Submarine fan development by cyclic sedimentation. *Marine Geology*, **20**, 27–40.

Maldonado, A. & Stanley, D. J. 1978. Nile Cone depositional processes and patterns in the Late Quaternary. *In*: Stanley, D. J. & Kelling, G. (eds) *Sedimentation in Submarine Canyons, Fans, and Trenches*. Dowden, Hutchinson & Ross, Stroudsburg, PA, 239–257.

Mart, Y. 1993. The sedimentologic and geomorphic provinces of the Nile Fan. *In*: Rhodes, E. G. & Moslow, T. S. (eds) *Marine Clastic Reservoirs*. Springer, New York, 101–112.

Mutti, E., Ricci Lucchi, F., Seguret, M. & Zanzucchi, G. 1984. Seismoturbidites: a new group of resedimented deposits. *Marine Geology*, **55**, 103–116.

Reeder, M. S., Rothwell, R. G. & Stow, D. A. V. 2000. Influence of sea level and basin physiography on emplacement of the late Pleistocene Herodotus Basin Megaturbidite, SE Mediterranean Sea. *Marine and Petroleum Geology*, 17, 199–218.

Reeder, M. S., Rothwell, R. G., Stow, D. A. V., Kahler, G. & Kenyon, N. H. 1998. Turbidite flux, architecture and chemostratigraphy of the Herodotus Basin, Levantine Sea, south-eastern Mediterranean. *In*: Stoker, M. S., Evans, D. & Cramp, D. (eds) *Geological Processes on Continental Margins: Sedimentation, Mass Wasting and Sability*, Geological Society, London, Special Publications, **129**, 19–41.

Ricci Lucchi, F. & Valmori, E. 1980. Basin-wide turbidites in a Miocene, over-supplied, deep-sea plain: a geometrical analysis. *Sedimentology*, **27**, 241–270.

Rohling, E. J. 1994. Review and new aspects concerning the formation of Eastern Mediterranean Sapropels. *Marine Geology*, **122**, 1–28.

Ross, D. A., Uchupi, E., Summerhayes, C. P., Koelsch, D. E. & El Shazly, E. M. 1978. Sedimentation and structure of the Nile Cone and Levant Platform area. *In*: Stanley, D. J. & Kelling, G. (eds) *Sedimentation in Submarine Canyons, Fans and Trenches*, Dowden, Hutchinson and Ross, Stroudsburg, PA, 261–275.

Said, R. 1990. Geomorphology. *In*: Said, R. (ed.) *The Geology of Egypt*. A. A. Balkema, Rotterdam, 9–25.

Shackleton, N. J. 1987. Oxygen isotopes, ice volume and sea level, *Quaternary Science Reviews*, **6**, 183–190.

Stanley, D. J. & Maldonado, A. 1979. Levantine Sea – Nile Cone lithostratigraphic evolution: Quantitative analysis and correlation with paleoclimatic and eustatic oscillations in the Late Quaternary. *Sedimentary Geology*, **23**, 37–65.

Stuiver, M. 1990. Timescales and telltale corals. *Nature*, **345**, 387–388.

Thomson, J. & Weaver, P. P. E. 1993. An AMS radiocarbon method to determine the emplacement of recent deep-sea turbidites. *Sedimentary Geology*, **89**, 1-7.